Miniaturization of Compact Quadrifilar Helix Antennas for Telemetry, Tracking and Command Applications

Alexandru Takacs[1,2], Hervé Aubert[1,3], Daniel Belot[4], Hubert Diez[4]
[1] CNRS, LAAS, 7 avenue du colonel Roche, F-31400, Toulouse, France
[2] Univ de Toulouse, UPS, LAAS, F-31400, Toulouse, France
[3] Univ de Toulouse, INP, LAAS, F-31400, Toulouse, France
[4] CNES (French Space Agency), Toulouse, France
e-mail: atakacs@laas.fr, aubert@laas.fr, daniel.belot@cnes.fr, hubert.diez@cnes.fr

***Abstract*—This paper addresses the miniaturization of Quadrifilar Helix Antennas (QHAs) for space applications (VHF Telemetry, Tracking and Command). Several shape miniaturization techniques were presented and the impact of height reduction is quantified in terms of radiation pattern, gain and phase center. Simulation and experimental results demonstrate that Compact Quadrifilar Helix Antennas (CQHAs) with a height reduced up to 70% reported to the reference QHA can be designed. By using an appropriate optimization method the impact of the miniaturization on CQHA performances in terms of radiation pattern and polarization purity can be minimized. Moreover the impact on the gain is quantified and design rules are reported. Finally a closed-form expression for estimating the gain of CQHAs from the height reduction factor is found.**

Keywords: compact antenna, Quadrifilar Helix Antenna, satellite antennas, miniaturization techniques

1. INTRODUCTION

QUADRIFILAR HELICAL ANTENNA (QHA) is formed by four helical antennas wound around the same longitudinal axis [1]. Each helical antenna is rotated 90° with respect to one another. This 60-years old antenna is naturally convenient for radiating circularly-polarized waves with a large variety of radiation patterns and radiation modes. Compared with the (monofilar) helical antenna QHAs are a new class of antennas allowing better performances mainly in terms of maximum gain,(circular) polarization purity and phase center stability. Most of QHA designs require a ground plane perpendicular on the longitudinal axis of the helical antennas. The input ports can be located on the ground side (bottom side of the QHA) or at the opposite ends (top side of the QHA). Open-ended or short-circuited QHA can be designed if the unfed ends are open-ended or short-circuited. The input ports can be fed with equal amplitude, clockwise or counterclockwise, in phase quadrature with a phase progression of +90° (direct) or -90° (reverse) between two consecutive ports. Thus forward or backward wave can be generated by properly controlling the wounding sense of the helical antennas and the phase progression of the input signals.
QHAs are resonant structures and the length of each constitutive helical antenna is multiple of the quarter wavelength. QHAs can be manufactured using wires or by using printed techniques. The wire is more suitable for low-frequency applications (VHF band) while the printed techniques are widely used for high-frequency applications (UHF or upper bands). The inherent properties of the QHAs (purity of the circular polarization, easily shaping of the radiation pattern and circularly-polarized radiated fields over a wide beamwidth) qualified QHA as an ideal candidate for satellite applications especially for Telemetry, Tracking and Command (TTC) applications. VHF QHAs are quite long antennas and, as other traditional antennas (e.g. parabolic antennas) QHAs face today to accommodation issues in the modern cost-effective satellite launch configuration. Consequently the miniaturization without significant degradation of radiation characteristics is the major challenge for any modern QHA design. QHAs are composed by four monofilar helical antennas.

The compact QHA reported in this paper are planned to be used for a telemetry link in VHF band on board of the satellite Space-based Multi-band Variable Object Monitor (SVOM), a science satellite project developed in bilateral cooperation between the French Space Agency (CNES) and the Chinese Space Agency. Several CQHA designs compatible with TTC requirements are presented here in order to analyze the impact of the miniaturization technique on antenna key parameters such as radiation

patterns, antenna gain and phase center stability. Measurement results are reported for experimental validation purposes. The design of standard QHA is summarized in Section 2. The adopted miniaturization technique and the CQHA design are presented in Section 3. The obtained experimental and simulation results of CQHAs are discussed in Section 4 with a focus on the impact of the miniaturization technique on the antenna gain.

2. QHA DESIGN

VHF QHAs are mainly used for low data rate telemetry link in the satellite communication systems. The key descriptors of QHA are the radius *r* of the helix (the radius of the supporting cylindrical structure), the pitch angle α (or alternatively the number *n* of the turns can be used) and the height *h* of the antenna (the height of the supporting cylindrical structure if it is used). The combination between the pitch angle, antenna height and antenna radius determines the antenna radiation characteristics. Fig. 1 shows a 3D simulation model of an open-ended QHA for $n<1$, the geometrical descriptors and relationship between n, α, r, h and l, where l denotes the total length of a single helical wire and, the simulated 3D radiation patterns (gain) of a short-circuited QHA. The length of the helical wire typically set the resonant frequencies and is approximately an integer multiple of the quarter wavelength. λ/4 or 3λ/4 configurations are generally used for the open-ended QHA while λ/2 or λ configurations are often used for short-circuited QHA. Other key parameters impacting QHA design and performances are the diameter d_g of the ground plane and the wire radius for wire-supported QHA (or the strip width for printed QHA). Wire-supported QHA designs were reported in [2]-[9] while printed QHA were studied in [10]-[15].

QHAs are mainly implemented on cylindrical surfaces (helical wires or strip lines are rolled up on cylindrical surfaces). However QHAs can be conformed on conical [16], spherical [17] or square [18] surfaces.

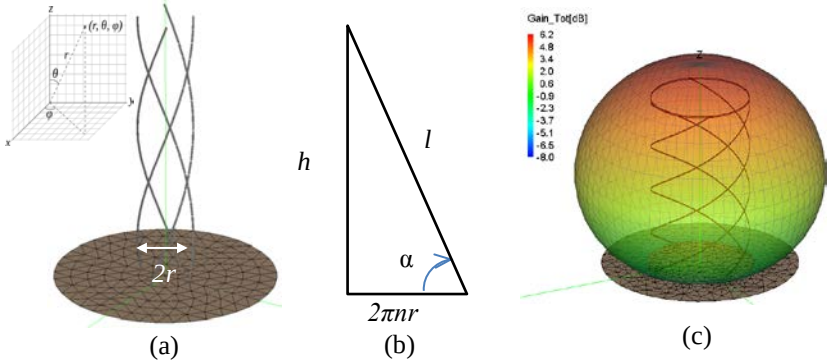


Figure 1. (a) air-supported simulation model (FEKO) for an open-end QHA including the finite-sized ground plane (the inset illustrates the adopted system of coordinates); (b) the geometrical relationship between the key descriptors of QHAs; (c) simulated (FEKO) 3D radiation pattern (gain, in dB) for a typical short-circuited QHA (axial mode).

Compact design is required for space application in order to fit the launch constraints. Thus quarter wavelength/half wavelength configurations are preferred despite of their well-known poor input matching (especially for the quarter wavelength design). The poor input matching can be compensated by the feeding network that operates, in most of cases, as a matching network. The feeding/matching network is not discussed in this paper.

Two designs for TTC space applications, called here QHA1 and QHA2, were selected as reference QHAs. These antennas are planned to be used for a telemetry link in VHF band on board of the SVOM satellite [19]. QHA1 is an open-ended quarter-wavelength QHA designed for operating at 137 MHz while QHA2 is a short-ended half-wavelength QHA operating at 162 MHz. Both of them radiate circularly-polarized electromagnetic fields in the so-called *axial mode* (the maximum power is radiated along the positive Oz direction). The main descriptors of these two reference QHAs are reported in Table I.

TABLE I
GEOMETRICAL DESCRIPTORS OF REFERENCE ANTENNAS QHA1 AND QHA2

		α	r(mm)	dg(mm)	h(mm)	l(mm)
QHA1	value	70°	50	400	514	547
	normalized to wavelength		0.05	0.18	0.24	0.25
QHA2	value	33°55’	125	500	450	930
	normalized to wavelength		0.07	0.27	0.24	0.50

3. MINIATURIZATION TECHNIQUES AND CQHA DESIGN

A. Miniaturization Techniques

Several miniaturization techniques were proposed in order to implement CQHA. Those techniques can be classified as follows:

(i) *shaping-based technique*: the helical wires are shaped in order to reduce the axial height of the helix while keeping almost unchanged the total length of the wires and consequently, the operating frequency;

(ii) *dielectric-loading technique*: a dielectric with medium/high dielectric constant is used as a cylindrical support for the CQHA and consequently, shorter wires (and smaller axial height) are used to operate at the desired frequency.

These two techniques can obviously be combined. The dielectric-loading technique facilitates the manufacturing process but the radiation efficiency can be drastically degraded because of the dielectric loss. For this reason the shaping-based technique is preferred here for miniaturizing the reference antennas QHA1 and QHA2 while keeping unchanged the radiation properties.

B. Quadrifilar Helix Antenna with Arbitrary Shape

In the past years the shape of constitutive wires in CQHAs were described by sinusoidal [6][12][15], periodic triangular [20], periodic trapezoidal [20], rectangular [12][21], meandered [13][14], pre-fractal [22], non-linear functions [23] and more recently, by the combination of fractal and sine functions [24] (a review of the patents on CQHAs can be found in [25]). The axial height of the QHA can be also reduced by modifying the geometry/the shape at the center of the helical section [7]-[8].

CQHA with an arbitrary wire shape can be modeled by the following system of parametric equations:

$$\begin{cases} x(t_{i+1}) = r\cos(\theta_i) \\ y(t_{i+1}) = r\sin(\theta_i) \qquad i \geq 1 \\ z(t_{i+1}) = t_{i+1}\sin(\alpha) + f(t_{i+1})\cos(\alpha) \quad , \end{cases} \tag{1}$$

$$\begin{cases} \theta_i = \dfrac{\sum_{j=1}^{i-1}\left[g(t_{j+1}) - g(t_j)\right]}{R} = \dfrac{g(t_i) - g(t_1)}{R}, i \geq 1 \\ g(t) = t\cos(\alpha) - f(t)\sin(\alpha), \quad t \in \Re \quad , \quad t \in [0, t_{\max}] \end{cases} \tag{2}$$

where t is a positive real number, t_{max} denotes the solution of the equation $h=z(t_{max})$ and $f(t)$ designates an arbitrary function called the *shaping function*. Eq. (1) allows computing numerically each point of the CQHA as function of the angular coordinate θ_i. By choosing the real-valued numbers t_i it is possible to adjust the number of points that controls the shape of helical wires of CQHA. A standard Cartesian coordinate system is adopted here with the origin sets at the center of the ground plane. The first point $(\theta_i=0°)$ of the helical wire is positioned at $x(0)=r$, $y(0)=0$ and $z(0)=0$. A helical wire for QHA/CQHA is generated by using Eqs. (1) and (2). The three other constitutive helical wires of the QHA or CQHA are derived from a standard rotation over the z-axis with 90°, 180° and 270° of the first helical wire. The shaping function of the reference QHA is given by:

$$f(t) = t \tag{3}$$

while CQHAs with a sinusoidal profile (i.e., with wires mathematically described by a linear combination of n sine functions) are such that:

$$f(t) = \sum_{j=0}^{n-1} A_j \sin(\omega_j t) \tag{4}$$

where A_j et ω_j denote the geometrical descriptors of the sinusoidal profile and can be viewed as amplitude and pulsation coefficients, respectively. Fractal shapes are generally not defined from closed-form expressions but are the result of an iterative process which can be further implemented inside most electromagnetic software. In order to obtain smaller structures the so-called *modified fractal profiles* (e.g., modified Von Koch or Peano) may be advantageously used. The procedure for modifying standard fractal shapes is detailed in [24] and [27]. These modified fractal profiles can be combined with a sine function as reported in [24] and [27] in so-called *Sine-Modulated Modified Fractal* (SMMF) profiles.

From a manufacturing point of view it can be convenient to print the shape of the helical wire (antenna) in a 2D plane and then to roll-up the printed 2D shape around a cylindrical supporting structure to form the CQHA. Fig. 2 illustrates 2D printed surfaces using various profiles and the corresponding 3D simulation models (FEKO) for CQHA. A periodicity is added into the design by

duplicating the elementary cell along each constitutive helical antenna. For example the cell appears twice in Fig. 2(a) while in Fig. 2(b) it is repeated four times. This periodicity (or number of cells) is an additional design parameter and is advantageously used during the optimization process.

C. Optimization Methodology

Miniaturizing QHA may impact the intrinsic antenna radiation performances. For TTC space applications it is mandatory to keep unchanged the radiation pattern and polarization purity. As the height of QHA becomes smaller the antenna gain decreases. Depending on the application and the overall power budget link lower gain can be increased by adding power amplifiers. However the modification of the radiation pattern due to the antenna miniaturization cannot be easily compensated.

A good trade-off between compactness, directivity, input matching, antenna gain and efficiency can be obtained by using an adequate optimization methodology.

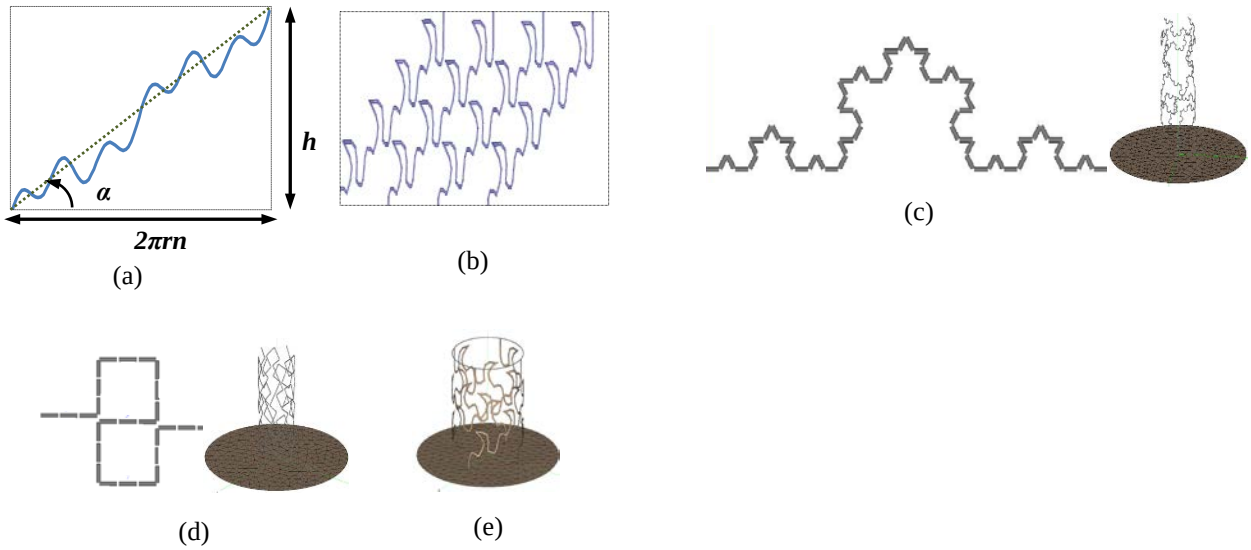


Figure 2. Some CQHA shapes considered in this paper: (a) a 2D shape combining multiple sine functions (continuous line) before rolling it up for generating a compact helical antenna; (b) four metallic strips having a Von Koch SMMF profile printed on a planar surface before rolling it up for generating a CQHA ; (c) prefractal Von Koch profile and the resulting CQHA 3D simulation model (FEKO); (d) prefractal Peano profile and the resulting CQHA 3D simulation model (FEKO); (e) 3D simulation model (FEKO) for a CQHA with a Von Koch SMMF.

In order to find the best fitted CQHA, an optimization process has been implemented using the optimization module of FEKO software. The following objective (goal) function *GF* has been defined in CADFEKO (OPTFEKO):

$$
\begin{aligned}
&GF = w_1 \cdot GF_1 + w_2 \cdot GF_2 + w_3 \cdot GF_3 + w_4 \cdot GF_4 ; \\
&GF_1 : S_{11} < 0.3 \\
&GF_2 : \text{LHC}\ (D) > 0\text{dB} \qquad \text{for} -60° \le \theta \le 60°, \quad \forall\phi \\
&GF_3 : \text{RHC}\ (D) < -10\text{dB} \qquad \text{for} -180° \le \theta \le 180°, \quad \forall\phi \\
&GF_4 : G_{max} > 0\text{dB}
\end{aligned}
\tag{5}
$$

where w_1, w_2, w_3 and w_4 are weight coefficients (positive real numbers), *LHC* and *RHC* designate respectively the left-handed and right-handed circular components of the directivity, S_{11} denotes the magnitude of the reflection coefficient at each port of the CQHA, G_{max} is the maximum gain of CQHA. The goal function *GF* is computed at the desired operating frequency, that is, (i) at 137MHz for QHA1 and CQHAs derived from QHA1 and, (ii) at 162 MHz for QHA2 and CQHAs derived from QHA2. The TTC technical specifications in VHF band require main polarization (LHC) of the reference QHA to be positive for $-60° \le \theta \le 60°$ while the cross-polarization (RHC) level is required to be lower than -10dB for $-180° \le \theta \le 180°$. Consequently the goal function *GF* intends to maintain the impedance matching (*GF1*), radiation pattern and polarization purity (*GF2* and *GF3*) at the same level than the reference antenna. This allows facilitating the comparisons between radiation performances of optimized CQHAs and will force the best-fitted CQHAs to fulfill the typical technical requirements for TTC applications. In Eq.(5) a fourth goal is targeted for classifying the designed CQHA in terms of maximum gain criteria. For TTC application it is not convenient to use antennas with negative gain (in dBi) and consequently, $G_{max}>0dBi$ is required as an additional goal *GF4*. The optimization

process uses the *Grid Search Method* implemented in FEKO and is based on the methodology described in [6] and [26]. Thousands of CQHAs based on sinusoidal, standard or modified prefractal and, SMMF [24] [27] profiles were chosen for optimization purposes. The obtained results are summarized and discussed in the next section.

4. CQHA: Results and Discussion

To demonstrate the concept and evaluate the impact of the miniaturization process on the antennas performances two approaches were applied. On one hand the wire-supported QHA1 and optimized CQHAs were manufactured using a low-cost technique based on a PVC tube (3mm thick) for the cylindrical supporting structure [28][29]. PVC has a relative dielectric permittivity close to 4 and high dielectric losses (dielectric loss tangent is around 0.06 [30]). On the other hand the printed QHA2 and the optimized CQHAs were manufactured using: (i) either a paper substrate (relative dielectric permittivity close to 3 and thickness of 0.15mm) and a quasi-printed technique [27] or (ii) the Dupont Melinex 339 PET dielectric (relative dielectric permittivity close to 3, loss tangent 0.007 and thickness of 0.1mm) and the commercially available technology from Inkjetflex [31]. Wire-supported QHA1 and a set of five CQHAs derived from QHA1 are shown in Fig. 3 while printed QHA2 and CQHAs derived from QHA2 are shown in Fig. 4.

Taking into account the dielectric supporting structure in the simulation model increases significantly the computational time. For instance the air-supported CQHA (i.e., without the cylindrical dielectric supporting structure) can be simulated in less than one minute on a PC with quad-core processor Intel Q9300 and 4GB of RAM, while the PVC-supported CQHA requires at least one hour. The computational time is a critical issue in the design/optimization process because thousands of CQHAs need to be computed here for finding the best-fitted CQHAs. In order to minimize the simulation time, the optimization was performed by using air-supported CQHA. Consequently simulation and optimization results reported in this paper concern antennas without the cylindrical supporting structure. However, in order to predict the eventual impact of such structure on antenna performances electromagnetic simulations have been performed by taking into account this structure only for the optimized designs selected for the manufacturing. Adding dielectric (supporting tube or thin film) decreases more or less the operating frequency and degrades the antenna efficiency and gain. This effect is found to be critical for wire-supported CQHA using thick PVC tube and is found to be not significant for printed CQHA printed on thin dielectric film.

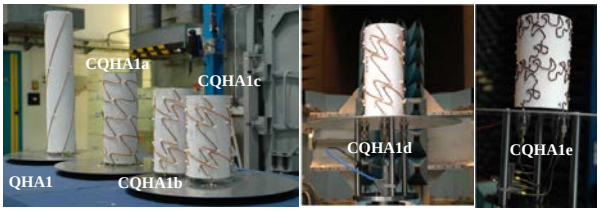


Figure 3. Manufactured wire-supported CQHAs derived from QHA1 using as shaping function various combinations of sine functions (CQHA1a, CQHA1b, CQHA1c and CQHA1d) and prefractal (Von Koch) profile combined with a sine function (CQHA1e).

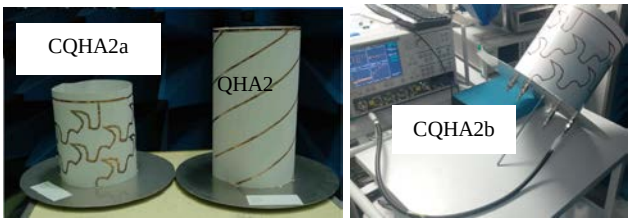


Figure 4. Manufactured printed CQHAs derived from QHA2 using a Von Koch-based SMMF as shaping function. CQHA2a was fabricated using the quasi-printed home-made technique on paper substrate while CQHA2b was manufactured using the commercially available technology from Inkjetflex.

A. Measurement Technique

The reflection coefficient at the input ports of the antennas was measured by using an Anritsu 37369C Vector Network Analyzer. When the reflection coefficient at one port is measured the unfed three other ports are loaded by 50Ω. The radiation pattern measurement in the VHF band is not an easy task and near field techniques are required. Radiation patterns have been measured by the French Space Agency using spherical near field measurement technique. In order to evaluate the antenna gain the reference Lindgren dipole [32] over a ground plane was used.

B. Simulation and Experimental Results

As previously explained the wire-supported antennas (QHA1 and the CQHAs derived from QHA1) have been designed/optimized without taking into account the cylindrical PVC supporting structure. Consequently the initial operating frequency was down-shifted from 137 MHz to approximately 120 MHz depending on the specific design. Five best-fitted wire-

supported CQHAs were manufactured and characterized. Their characteristics are summarized in Table II.

In order to compare the performances of overall manufactured antennas the operating frequency of 120 MHz was selected for measuring the radiation patterns. The electromagnetic simulations indicate that the polarization purity and the shape of the radiation pattern are not significantly modified compared with the reference antenna in a 10% bandwidth centered at the resonant frequency. Table II demonstrates experimentally that CQHAs with a height reduced up to 70% reported to the reference QHA can be designed.

TABLE II
QHA1/ CQHA1 MEASURED CHARACTERISTICS

Antenna name	Height (mm)	Relative height (%)	Measured S_{11} (dB)	Measured directivity (dBi)	Shaping function f(t)
QHA1	514	100	-6.2 at 123 MHz	5.9	Straight line
CQHA1a	270	52.5	-8.1 at 120 MHz	5.6	Sinusoidal
CQHA1b	217	42	-8.3 at 118 MHz	5.6	Sinusoidal
CQHA1c	193	37.5	-8.6 at 115 MHz	5.4	Sinusoidal
CQHA1d	135	26.2	-7.6 at 119 MHz	5.6	Sinusoidal
CQHA1e	167	32.5	-9.5 at 125 MHz	5.2	Von Koch SMMF

Fig. 5 shows the measured and the simulated LHC and RHC components of the directivity for the reference QHA1 at 120 MHz. These results demonstrate that TTC requirements given by Eq.(5) regarding the radiation pattern and the polarization purity are fulfilled by QHA1. As expected the maximum directivity (5.9dBi) was measured for $\Phi=\theta=0°$.

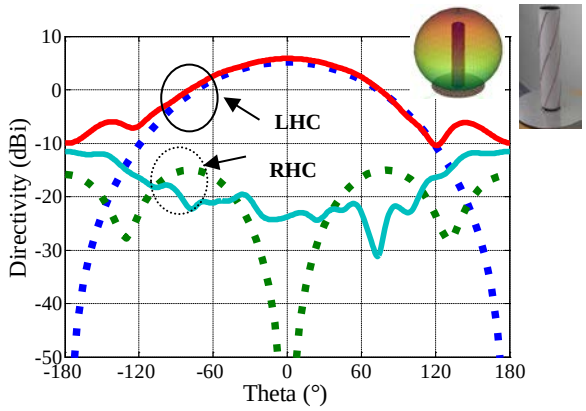


Figure 5. Experimental (continuous line) and simulated using FEKO (dashed line) results for the radiation pattern (Φ=0°) for the PVC-supported reference QHA1 at 120MHz. The insets give the 3D simulated radiation pattern (directivity) and the photography of the manufactured QHA1 prototype.

Fig. 6 shows the normalized gain (QHA1 is taken as reference results) for CQHA1a, CQHA1b, CQHA1c and CQHA1d. The gain is significantly impacted when the height of the antenna decreases because the helix radius is quite small in this work and consequently, a strong electromagnetic coupling occurs between the constitutive helical antennas. This coupling is also favored by the PVC supporting cylindrical structure.

Fig. 7 reports the simulated gain of CQHAs as a function of the antenna relative height for various wire profiles. The relative height is denoted R_H and is defined as the ratio between the height of the CQHA and height of the reference QHA. Each point of the curves reported in Fig. 7 corresponds to the best-fitted CQHA obtained by using the optimization methodology described in Section 3.C.

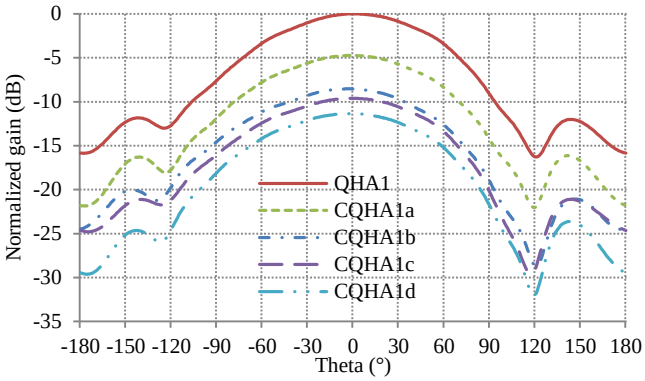


Figure 6. Measured gain of the CQHA relative to the measured gain of the QHA1 (frequency: 120 MHz).

Typically thousands of candidates were tested in order to derive only the best-fitted solution. Moreover the optimization process based on the goal function described by Eq. (5) may not bring acceptable solutions for a given profile and a given relative height. For example the Von Koch profile does not provide solution (fitted to the goal function) for $R_H < 55\%$.

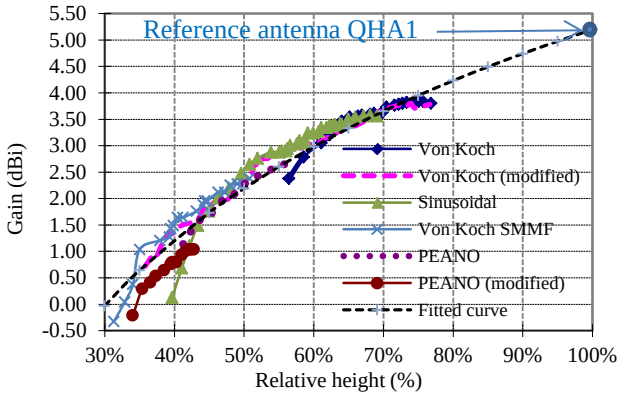


Figure 7. Gain of best-fitted CQHAs (regarding the goal function defined by Eq.(5)) as a function of the antenna relative height for various wire profiles (simulated results). The dashed curve fits all the data reported in this figure.

The goal function *GF4* defined in Eq. (5) requires $G_{max} > 0\ dBi$. Thus the best-fitted CQHAs reported in Fig. 7 are such that $G_{max} > -0.5\ dBi$ and consequently, the relative height compared with the reference antenna QHA is higher than 30%. For relative height higher than 60% basically the same gain for all the analyzed profiles was found. Prefractal shapes provide no solution to Eq. (5) for relative height lower than 55 % (Von Koch) or 40% (Peano). For obtaining smaller structures the modified fractal profiles (e.g., modified Von Koch or Peano profiles) may be used. Moreover sinusoidal profiles can be advantageously used when a relative height ranging from 40% to 90% is required but, the gain is significantly reduced when the relative height is lower than 45%. Modified fractal shape is a better choice in this case as it allows obtaining higher gain. From Fig. 7 it can be observed that the combination of modified fractal profile with a sine function allows maximizing the gain for very compact CQHAs (i.e., for relative height lower than 40%). As shown in Fig. 7 lower limits exist for the relative height. These lower limits depend on the chosen objective goal function (see eq. 5). For a given goal function and for a given CGHA profile these limitations are caused by: (i) the overlapping between close wires (geometrical limitation) and (ii) the increase of the electromagnetic coupling between the constitutive helical wires of the CQHA that increases the amount of the electromagnetic energy stored by the CQHA.

Surprisingly, whatever the chosen profile or shaping function, all the best-fitted solutions reported in Fig. 7 seem to follow a simple law described by the following closed-form expression:

$$G_{CQHA}(\text{dBi}) = 10 \cdot \log(R_H) + G_{QHA}(\text{dBi}) \qquad \text{(6-a)}$$

or equivalently:

$$\frac{G_{CQHA}}{G_{QHA}} = \frac{h_{CQHA}}{h_{QHA}} = R_H \qquad \text{(6-b)}$$

where G_{QHA} and G_{CQHA} denote respectively the gain of the reference antenna QHA and the gain of the CQHA and, h_{QHA} and

h_{CQHA} designate respectively the height of QHA and the height of CQHA. The physical interpretation of Eq.(6) is not obvious. For obtaining the numerical data reported in Fig. 7 thousands of CQHA based on six different shapes (sinusoidal, Von Koch, Peano, Von Koch modified, Peano modified, and Von Koch SMMF profiles) and with various geometrical descriptors were numerically simulated by using the methodology described in Section 3.C. Hundreds of best fitted CQHAs were selected according to the goal function Eq.(5) and reported in Fig. 7. Eq.(6) can be very useful in practice: for a given antenna height (or R_H) the designer can predict the gain achievable by a CQHA, check if the resulting compact antenna fulfills the launch system requirement and decide if the proposed CQHA is suitable for the TTC system.

The impact of the miniaturization process on the wire supported CQHA was investigated by the authors in [26] with a focus on the phase center stability. Exact location of the phase center is crucial mainly for high resolution GPS (Global Positioning Systems) application. As expected the phase center of QHAs/CQHAs is always located on the symmetry axis of CQHAs and positioned below the phase center of the QHA. As a general rule the phase center approaches the antenna ground plane as the height reduction increases [26]. The position of the phase center is in the range of CQHA height for moderate reduction size factor and can slightly exceed the antenna height for very compact CQHAs.

Printed QHA/CQHA were designed and manufactured. Their characteristics are summarized in Table III.

TABLE III
QHA2/ CQHA2 MEASURED CHARACTERISTICS

	h (mm)	Relative height (%)	f_0 (MHz)	S11 (dB)	D_{max} (dBi)	G_{max} [1] (dBi	G_{max} [2] (dBi
QHA2	450	-	162	-13	6.4	2.37	6
CQHA2a	265	58.8	161.3	-10	5.4	-1.3	2
CQHA2b	262	58.2	159.4	-14	N/A[3]	N/A	N/A

[1] the insertion loss of the feeding network is included in this gain
[2] the insertion loss of the feeding network is de-embedded
[3] not available before the submission deadline of this paper

The compact structures CQHA2a and CQHA2b are based on a modified Von Koch shape combined with a sine function because this profile leads to higher gain for very compact CQHA (i.e., when the relative height is lower than 50%). As expected the down-shift of the operating frequency is reduced in this case because a thinner dielectric substrate (0.15mm instead of 3 mm) with lower dielectric constant (3 instead of 4) were used as a cylindrical supporting structure instead of a PVC tube. The measured operating frequency f_0 is reported in Table III.

In order to perform one port radiation pattern measurement of the CQHAs a feeding network based on commercially available couplers and phase shifters was fabricated. The average insertion loss of the feeding network was found to be 3.7dB with a minimum reflection coefficient at the antenna terminals of -35dB at 155MHz. The measured phase progression between two adjacent ports at the output of the feeding network (the input of the QHA2/CQHA2) is 91.6° (port 1 to 2), 90.8° (port 2 to 3) and 89.8° (port 3 to 4) respectively. Fig. 8 shows the simulated co-polarization (LHC) and cross-polarization (RHC) components of the gain for QHA2 and CQHA2 at 162 MHz. As represented in Fig. 8 CQHA2 fulfill the requirements for a TTC application as implemented by the goal function (Eq. 5). The supporting thin dielectric film (paper for CQHA2a and PET for CQHA2b) was not taken into account in the simulation model.

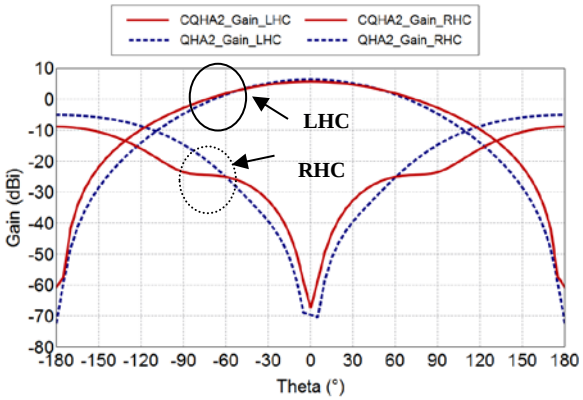


Figure 8. Simulated co-polarization (LHC) and cross-polarization (RHC) components of the gain for the reference antenna QHA2 and the compact antenna CQHA2a.

Fig. 9 shows the measured directivity (LHC and RHC components) of CQHA2a as a function of angle θ for two cut planes: ϕ=0° and ϕ=90°.

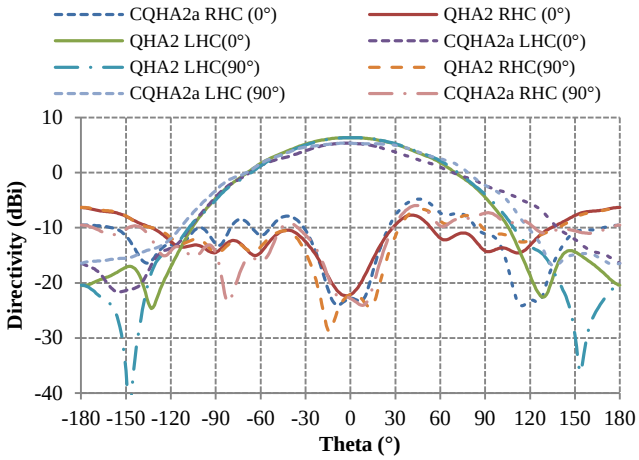


Figure 9. Measured co-polarization (LHC) and cross-polarization (RHC) components of the directivity for the references antenna QHA2 and the compact antenna CQHA2a as function of theta angle (°) for phi=0° (xOy) and phi=90°.

The differences observed in these planes are mainly caused by the manufacturing process. There are more important for cross-polarization components (RHC) and are negligible for the co-polarization component (LHC) in the targeted beamwidth -60°≤θ≤60°. The CQHA2b should minimize these discrepancies because a symmetrical structure was fabricated using a more reliable fabrication technology. No measurement was performed on CQHA2b before the submission deadline of this paper but the electromagnetic simulation demonstrates performances similar to ones obtained for CQHA2a.

5. Conclusion

Simulation and experimental results demonstrate that CQHAs with an axial height reduced up to 70% reported to the reference QHA can be obtained by using various shape profiles and an appropriate optimization method. The impact of the miniaturization on CQHA performances in terms of radiation pattern and polarization purity can be controlled and minimized in order to fulfil the technical requirements of a VHF TTC system. It was shown that the choice of the shape profile is not critical when relative height higher than 60% is required. Moreover few profiles (e.g. standard prefractal profiles such as Peano and Von Koch shapes) cannot provide very compact structures. The impact of the shape is critical on the gain for very compact quadrifilar helix antennas (i.e., when relative height lower than 40% is required). In order to estimate the gain achievable by CQHA a practical closed-form equation, very useful from a system design point of view, was derived from extensive numerical data. It was established that, whatever the chosen profile, the gain of CQHA normalized by the gain of the reference QHA equals to the height of the CQHA normalized by the height of the QHA.

Acknowledgments

This work was supported in part by the CNES (French Space Agency) under the grant Ref. DCT/RF/AN – 2011.0011001 (2011) and DCT/RF/AN – 2009.0009307 (2009).

The authors acknowledge the technical support of Xavier Dollat and Antony Coustou (CNRS-LAAS), Tonio Idda (former CNRS-LAAS), Emanouil Koufidakis and Nelson Fonseca (former CNES), Mingtian Wang (University of Toulouse) and Mohamed Fodil (former University of Toulouse) for their contributions in the different phases of this research work.

References

[1] C.A. Balanis, *Modern Antenna Handbook*, John Willey & sons, 2008, pp. 455-457.
[2] C.C. Kilgus, "Resonant quadrifilar helix," *IEEE Trans. on Antenna and Propagation*, May 1969, Vol. 17, Issue 3, pp 349 – 351.
[3] C.C. Kilgus, "Multielement, fractional turn helices," *IEEE Trans. on Antenna and Propagation*, July 1968, Vol. 16, Issue 4, pp. 499 – 500.
[4] C.C. Kilgus, "Resonant quadrifilar helix design, Technical Feature," *Microwave Journal*, December 1970, pp. 49 – 54.
[5] C.C. Kilgus, "Shaped-conical radiation pattern performance of the backfire quadrifilar helix," *IEEE Trans. on Antenna and Propagation*, May 1975, Vol. 23, Issue 3, pp. 392 – 397.
[6] A. Takacs, N. J.G. Fonseca, H. Aubert, "Height Reduction of the Axial-Mode Open-Ended Quadrifilar Helical Antenna", *IEEE Antenna and Wireless Propagation Letters*, vol. 9, pp. 942-945, 2010.
[7] M. Amin, R. Cahil, "Compact quadrifilar helix antenna"; *IET Electronics Letters*, June 2005, Vol. 41, No. 12, pp 672 – 674.
[8] M. Amin, R. Cahil, V.F. Fusco, "Mechanically Tunable Multiband Compact Quadrifilar Helix Antenna With Dual Mode Operation", *IEEE Trans. on Antenna and Propagation*, June 2008, Vol. 56, No. 6, pp. 1528-1532.
[9] M. Amin, R. Cahil, "Effect of Helix Turn Angle on the Performance of a Half Wavelength Quadrifilar Antenna", *IEEE Microwave and Wireless Propagation Letters, June 2006*, Vol. 16, No. 6, pp.384-386.
[10] A. Auriol, "Helix-type antenna and its manufacturing process," European Patent, publication number: 0320404A1, 14 June 1989

[11] A. Adams, R. Greenough, R.Wallenberg, A. Mendelovicz, C. Lumjiak, "The quadrifilar helix antenna," *IEEE Trans. on Antenna and Propagation*, Mar 1974, Vol. 22, Issue 2, pp. 173 – 178.
[12] M.G. Ibambe, Y. Letestu and A. Sharaiha, "Compact printed quadrifilar helical antenna," *IET Electronics Letters*, Vol. 43, Issue 13, pp: 697-698, 21 June 2007.
[13] D. K. C. Chew and S. R. Saunders, "Meander Line Technique for Size Reduction of Quadrifilar Helix Antenna," *IEEE Antennas and Wireless Propagation Letters*, Vol. 1, pp. 109-111, 2002.
[14] B. Bhandari, S. Gao and T. Brown, "Meandered Variable Pitch Angle Printed Quadrifilar Helix Antenna," in *Proc. of LAPC'2009*, Loughborough, UK, Nov. 16-17, 2009, pp. 325-327.
[15] L. Hanane, S. Hebib, H. Aubert and N.J.G. Fonseca, "Antenna of the Helix Type Having Radiating Strands with a Sinusoidal Pattern and Associated Manufacturing Process," Patent International Publication Number WO 2009/034125 A1, Mar. 19, 2009.
[16] J. Back, J. Zackrisson, M. Ohgren, P. Ingvarson, "A New Quadrifilar Helix Antenna Family with Flexible Coverage for Space Applications," in *Proc. of EuCAP 2007*, Edinburgh, UK, 11-16 Nov. 2007, pp: 1-6.
[17] A. Mirkamali, L. Akhoondzadeh, K. Keyghobad, M. Soleimani, "A novel Quadrifilar Helix Antenna For Use In LEO Satellite Communications," in *Proc. of International Conf. on Antenna Theory and Techniques*, Sevastopol, Ukraine,9-12 Sept., 2003, pp. 509-511.
[18] W. I. Son, W. G. Lim, M. Q. Lee, S. B. Min, J.W. Yu, "Printed Square Quadrifilar Helix Antenna (QHA) for GPS Receiver," in *Proc. of EUMC'2008*, Amsterdam, Netherlands, Oct. 2008, pp.1292-1296.
[19] http://smsc.cnes.fr/SVOM/Fr/GP_satellite.htm
[20] J. Inoue, "Helical Antenna," International Publication Number WO 01/24315, Apr. 4, 2001.
[21] S.R. Saunders and D. Kwan Chong Chew, "Multifilar Helix Antennas," US Patent 7,142,170 B2, Nov. 28, 2006.
[22] N. Fonseca, S. Hebib, H. Aubert and L. Hanane, "Helix Antenna," Patent International Publication Number WO 2008/142099 A1, Nov. 27, 2008.
[23] M. Ermutlu and K.K.-P. Kiesi, "Multi-filar Helix Antennae," US Patent 6,232,929 B1, May 15, 2001.
[24] H. Aubert, H. Diez, D. Belot, A. Takacs, "Compact helical antenna with a sinusoidal profile modulating a fractal pattern", Patent International Publication Number WO 2013139935 A1.
[25] N. Fonseca, H. Aubert, "Compact helical antennas – a review', *Recent Patents Electr. Eng. J.*, 2010, 9, pp. 942-945.
[26] A. Takacs, H. Aubert, H. Diez, D. Belot, „Miniaturization of Quadrifilar Helical Antenna: Impact on Efficiency and Phase Center Position", *IET Microwaves, Antennas & Propagation*, Vol. 7, Issue 3, 19 February 2013, pp. 202 – 207.
[27] A. Takacs, T. Idda, H. Aubert, H. Diez, "Compact VHF Quadrifilar Helix Antenna", in *Proc. of EUMC'2012*, Amsterdam, Netherlands, 28 Oct – 2 Nov. 2012.
[28] N.J.G. Fonseca, A. Takacs and H. Aubert, "Design and Experimental Validation of a Compact Quadrifilar Helix Antenna in VHF Band," in *Proc. of APMC 2009*, Singapore, Dec. 7-10, 2009.
[29] A. Takacs, N.J.G. Fonseca, H. Aubert and X. Dollat, "Miniaturization of Quadrifilar Helix Antenna for VHF Band Applications," in *Proc. of LAPC'2009*, Loughborough, UK, Nov. 16-17, 2009, pp. 597-600.
[30] Modern Plastics Encyclopaedia, 1981-1982, Mc Graw Hill, New York.
[31] www.inkjetflex.com
[32] http://www.ets-lindgren.com/3121D